Journal of Engineering Mathematics (2005) 52: 321–336
DOI 10.1007/s10665-005-2731-7

Variable-energy blast waves generated by a piston moving in a dusty gas

W. GRETLER and R. REGENFELDER
Institute of Fluid Mechanics and Heat Transfer, Technical University Graz, Austria (gretler@tugraz.at)

Received 16 June 2003; accepted in revised form 16 February 2005

Abstract. This paper presents a similarity solution for strong blast waves of variable energy propagating in a dusty gas. It is assumed that the equilibrium-flow condition is maintained and the variable energy input is supplied by a driving piston or surface according to a time-dependent power law. Three cases have been investigated: Case I corresponds to a decelerated piston, Case II to a piston of constant velocity, and Case III to a continuously accelerated piston starting from rest. Except in the case of constant front velocity, the similarity solution is valid for adiabatic flow as long as the effect of the counter-pressure is neglected. The effects of a parameter characterizing the various energy input of the blast wave on the similarity solution have been examined. The computations have been performed for various values of mass concentration of the solid particles and for the ratio of density of solid particles to the constant initial density of gas. Tables and graphs of numerical results are presented and discussed.

Key words: dust-laden flow, similarity solution, variable-energy blasts

1. Introduction

Similarity solutions for a strong blast-wave generated by the instantaneous energy release from a point source, a line source or a plane source in an ideal gas have been presented first by Taylor [1] and Sedov [2, pp. 154–191]. A detailed analytical investigation of a cylindrical blast wave with time-dependent energy input resulting from exploding wires was undertaken by Freeman [3]. Examples of time-dependent energy deposition are laser-driven blast waves, a chemical energy release occurring in a two-phase detonation, arc discharges and exploding wire phenomena. Laser-driven shocks with variable energy deposited at the center have been explored by Director and Dabora [4]. Dabora [5] found that the variable-energy case corresponds to the piston problem. The self-similar case of variable-energy deposition in the flow field for ideal gas was also treated by Guirgius *et al.* [6].

For a dusty gas with exponentially varying density, Vishwakarma [7] obtained a solution for the flow field caused by strong shock-wave propagation. But this solution is confined to a particular case in which the shock radius varies logarithmically in accordance with the special time dependence of the shock velocity. An analytical solution for the case of a planar dusty-gas flow with constant shock velocity generated by a piston moving with constant velocity was published by Miura and Glass [8] describing relaxation effects at small and moderate Mach numbers. Their results reflected only the effects of the additional inertia of the dust upon the wave propagation, since they assumed that the dust load has virtually a mass fraction but no volume fraction.

In the present paper, we present a similarity solution for the flow field behind the shock front and the inner expanding surface or piston moving with a velocity according to $u_p = ct^n$, where c and n are constants. As many authors studying particle-free flow followed Freeman's proposal [3], we also assumed that the total energy input depends on time as $E = Pt^{\beta}$, where P and β are taken as constants. For the analysis, we treat the adiabatic flow as a mixture of a gas and a pseudo-fluid at a velocity and temperature equilibrium with a constant ratio of specific heats of the mixture. This assumption may be a good approximation for strong shock waves, because the thickness of the relaxation zone behind the shock front, where the interaction between gas and particles through viscous drag and heat-transfer produces considerable deviations from velocity and temperature equilibrium, becomes very small for high Mach numbers. Recently, Saito *et al.* [9] have found that the transition-zone length for $10\,\mu$m in diameter spheres of grown glass (density $2500\,\mathrm{kg/m^3}$) for the frozen shock Mach numbers $M = 1{\cdot}2$ and $M = 3$ are 18 and 6·5 cm, respectively. Therefore, when the shock position is greater than 10 cm, the assumption of velocity and temperature equilibrium is quite justified for the case of strong blast waves, provided that the size of the particles is of the order $\leq 10\mu$m [12]. Pai *et al.* [10], [11, pp. 561–564] and Higashino [12] have already analyzed the problem of a strong blast wave under the assumption of velocity and temperature equilibrium and obtained similarity solutions. Shock waves of weak or moderate strength in a dusty gas were investigated by Rudinger and Chang [13], Marble [14], Higashino [15] and Geng and Grönig [16]. The propagation of shock waves in dusty gas has been studied for the last four decades to due their application to many engineering problems in industry and the environment. Blast-wave propagation in a dusty atmosphere and industrial explosions are important examples of such applications [16].

In the present study, numerical results are obtained for three different cases of spherical symmetry depending on the piston-velocity exponent n or on its counterpart, *i.e.*, on the energy-input parameter β. Both the position of the shock wave and the driving surface (piston face) are functions of time. The increase of the total energy of the flow between the shock front and the piston with time can be obtained by the pressure exerted on the mixture by the inner expanding surface. In addition, we will analyze how the mass concentration of the solid particles k_p and the ratio of the density of solid particles to the initial density of the gas affect the flow field behind the shock front. It is revealed that an increase in G increases the shock strength (effective shock Mach number). On the other hand, an increase in k_p decreases the shock strength for lower values of G (*e.g.*, $G = 1$), whereas higher values of G (*e.g.*, $G \geq 10$) lead to an increase. Also, this most striking effect of the dust-loading parameters will be discussed by means of physical parameters such as compressibility, additional inertia, and energy integral of the mixture.

It should be emphasized that the terminology "shock wave" could also be used here in all three cases to indicate the shock front, not the whole flow field, since a blast wave may be generally defined as the flow field behind a moving shock wave [3]. Because of this, the flow field in Case II corresponding to a piston of constant velocity is considered as a so-called constant-velocity blast wave [17], [18].

2. Basic equations

2.1. Conservation equations

The non-steady, one-dimensional flow field in a mixture of gas and small solid particles is a function of two independent variables, the time t and the space coordinate r. In order to get some essential features of shock-wave propagation, it is assumed that the equilibrium-flow condition is maintained in the flow field [10–12], [16]. If the stream cross-section A is independent of time, the conservation equations governing the flow can be expressed as

$$\frac{\partial \varrho}{\partial t}+u\frac{\partial \varrho}{\partial r}+\varrho\frac{\partial u}{\partial r}=-j\frac{\varrho u}{r}, \tag{1}$$

$$\frac{\partial u}{\partial t}+u\frac{\partial u}{\partial r}+\frac{1}{\varrho}\frac{\partial p}{\partial r}=0, \tag{2}$$

$$\frac{\partial e}{\partial t}+u\frac{\partial e}{\partial r}-\frac{p}{\varrho^2}\left(\frac{\partial \varrho}{\partial t}+u\frac{\partial \varrho}{\partial r}\right)=0, \tag{3}$$

where $u(r,t)$ is the velocity of the mixture, $p(r,t)$ the pressure of the mixture, $\varrho(r,t)$ the density of the mixture and $e(r,t)$ the internal energy of the mixture per unit mass. Further, the geometry factor j is defined by

$$j=\frac{\mathrm{d}\log A}{\mathrm{d}\log r}, \tag{4}$$

where $j=0$ for plane symmetry, $j=1$ for line symmetry, $j=2$ for point symmetry.

Due to the condition of velocity and temperature equilibrium, the terms of drag force and heat-transfer rate, which can be expressed via the drag coefficient and the Nusselt number, do not appear in the right-hand sides of Equations (2) and (3), [15], [16]. These terms are, of course, important for evaluating the extent of the relaxation zone behind the shock front which is, however, beyond the scope of this paper.

The equation of state of the mixture subject to the equilibrium condition is

$$p=\left(\frac{1-k_p}{1-Z}\right)\varrho R_i T, \tag{5}$$

where $k_p=m_{\mathrm{sp}}/m$ is the mass concentration of the solid particles (m_{sp}) in the mixture (m) taken as a constant in the whole flow field, Z is the volume fraction of the solid particles, R_i is the gas constant and T is the temperature. The relation between k_p and Z is given by Pai *et al.* [9] as

$$k_p=\frac{Z\varrho_{\mathrm{sp}}}{\varrho}, \tag{6}$$

where $Z=(Z_a/\varrho_a)\varrho$, while ϱ_{sp} is the species density of the solid particles and a subscript a refers to the initial values of Z and ϱ.

$$Z_a=\frac{V_{\mathrm{sp}}}{V_{\mathrm{ga}}+V_{\mathrm{sp}}}=\frac{k_p}{G(1-k_p)+k_p}, \tag{7}$$

where the volume of the mixture V is the sum of the volume of the perfect gas at the reference state V_{ga} and the volume of the particles V_{sp} which remains constant. The parameter G is defined as

$$G=\frac{\varrho_{\mathrm{sp}}}{\varrho_{\mathrm{ga}}}, \tag{8}$$

which is equal to the ratio of the density of the solid particles to the initial density of the gas. Hence, the fundamental parameters of the Pai model are k_p and G which describe the effects of the dust loading. For the dust-loading parameter G, we have a range of $G=1$ to $G\to\infty$, *i.e.*, $V_{\mathrm{sp}}\to 0$.

The internal energy of the mixture is related to the internal energies of the two species and may be written as

$$e = c_{vm}T = \left[k_p c_{\rm sp} + (1-k_p)c_v\right]T, \tag{9}$$

where $c_{\rm sp}$ is the specific heat of the solid particles, c_v the specific heat of the gas at constant volume and c_{vm} is the specific heat of the mixture at constant volume. For equilibrium conditions, the specific heat of the mixture at constant pressure is

$$c_{pm} = k_p c_{\rm sp} + (1-k_p)c_p, \tag{10}$$

where c_p is the specific heat of the gas at constant pressure. The ratio of the specific heats of the mixture is then

$$\Gamma = \frac{c_{pm}}{c_{vm}} = \frac{\gamma + \delta\beta_{\rm sp}}{1+\delta\beta_{\rm sp}}, \tag{11}$$

where $\quad \gamma = c_p/c_v, \quad \beta_{\rm sp} = c_{\rm sp}/c_v, \quad \delta = k_p/(1-k_p).$

Eliminating the temperature from (5), (7) and (9), we may write the internal energy of the mixture as follows:

$$e = \left(\frac{1-Z}{\Gamma-1}\right)\frac{p}{\varrho}. \tag{12}$$

The equilibrium sound speed of the mixture obtained by using the effective ratio of specific heats and effective gas constant $R_M = (1-k_p)R_i$ is

$$a_M = \left(\frac{\mathrm{d}p}{\mathrm{d}\varrho}\right)^{\frac{1}{2}} = \left(\frac{\Gamma}{1-Z}\frac{p}{\varrho}\right)^{\frac{1}{2}} = \left[\frac{\Gamma(1-k_p)R_iT}{(1-Z)^2}\right]^{\frac{1}{2}}. \tag{13}$$

Thus, the ratio of the equilibrium sound speed of the mixture to that of a particle-free gas is

$$\frac{a_M}{a} = \frac{1}{1-Z}\left[\frac{\Gamma}{\gamma}(1-k_p)\right]^{\frac{1}{2}} = \frac{1}{1-Z}\left[\frac{\left(1+\frac{\delta\beta_{\rm sp}}{\gamma}\right)(1-k_p)}{1+\delta\beta_{\rm sp}}\right]^{\frac{1}{2}}. \tag{14}$$

The deviation of the behavior of a dusty gas from that of a perfect gas is indicated by the compressibility defined as $\tau = 1/\varrho a_M^2$. The volume of the particles lowers the compressibility of the mixture, while the mass of the solid particles increases the total mass, and therefore may add to the inertia of the mixture. This can be demonstrated in two limiting cases of the mixture at the initial state. For $G=1$, it follows from Equations (7), (5) that $Z_a = k_p$, $\varrho_a = p_a/R_iT$ and $\tau = (1-k_p)/\Gamma_a p_a$, *i.e.*, the presence of the solid particles linearly lowers the compressibility of the mixture in the initial state. In the other limiting case, *i.e.*, for $G \to \infty$, the volume of the solid particles $V_{\rm sp}$ tends to zero. According to (7), the volume fraction Z_a is equal to zero. In this case, the compressibility $\tau = 1/\Gamma_a p_a$ is not effected by the dust loading. The solid particles contribute only to increasing the mass and inertia of the mixture.

2.2. Boundary conditions and energy integral

At the shock front, we have the usual equations for conservation of mass, momentum, and energy:

$$\varrho_a W_n = \varrho_n(W_n - u_n), \tag{15}$$

$$p_a + \varrho_a W_n^2 = p_n + \varrho_n(W_n-u_n)^2, \tag{16}$$

$$e_a + \frac{p_a}{\varrho_a} + \frac{W_n^2}{2} = e_n + \frac{p_n}{\varrho_n} + \frac{(W_n - u_n)^2}{2}, \tag{17}$$

where the subscript a refers to the values immediately in front of the shock, the subscript n refers to the values immediately behind the shock and W_n is the front-propagation velocity.

At the inner boundary of a blast wave generated by a piston, we have the condition

$$u_p = \left(\frac{\partial r}{\partial t}\right)_p. \tag{18}$$

The principle of global energy can be expressed in terms of the following integral relation:

$$\int_{r_p}^{r_n} \left(e + \frac{u^2}{2}\right) \varrho r^j \mathrm{d}r = \int_0^{r_n} e_a \varrho_a r^j \mathrm{d}r + \frac{P}{n_j} t_n^{\beta}. \tag{19}$$

In this model, β is the so-called energy-input parameter and P is a proportionality constant as mentioned above and n_j is a geometrical factor defined as $n_j = 2j\pi + (1/2)(j-1)(j-2)$. If the energy is supplied by a driving piston as in the present problem in which the flow is self-similar, the constant P can be made dimensionless. Using the density of the medium at rest and the constant c of the piston velocity, the non-dimensional constant is $P/\varrho_a c^{j+3}$, provided $(n+1)(j+3) = 2+\beta$, and its values may be found in Section 4 where the results are summarized in Table 1. Since the work done by the piston can be described by the same power law, we obtain for self-similar flow on the other hand $P/\varrho_a c^{j+3} = n_j p_p / \varrho_a {W_n}^2 (j+1)$.

Basically, Freeman's model is independent of whether the energy is absorbed at the shock front [19] (laser radiation), or within the flow field (piston) as in the present problem.

2.3. Conservation equations and boundary conditions in non-dimensional form

The basic equations can be made dimensionless by transforming the independent variables for space r and time t into new independent variables:

$$x \equiv \frac{r}{r_n} \quad \text{and} \quad \xi \equiv \frac{r_n}{R_o} \quad \text{or} \quad y \equiv \frac{a_a^2}{W_n^2} = \frac{1}{M^2}. \tag{20}$$

Here x and ξ are the so-called field coordinate and front coordinate, respectively. R_0 is a reference-front radius. R_0 depends on the two most important parameters of the problem, namely the energy-input parameter β and the pressure p_a of the undisturbed medium, and will be defined later on. The shock Mach number $M = 1/\sqrt{y}$ refers to the effective speed of sound $a_a = \sqrt{\Gamma p_a/(1-Z_a)\varrho_a}$ for the undisturbed medium.

Introducing new dependent variables defined by

$$f \equiv \frac{u}{W_n}, \quad g \equiv \frac{p}{\varrho_a {W_n}^2}, \quad h \equiv \frac{\varrho}{\varrho_a}, \quad \sigma \equiv \frac{e}{{W_n}^2} \tag{21}$$

and applying the operators

$$\frac{\partial}{\partial r} = \frac{1}{r_n}\frac{\partial}{\partial x}, \quad \frac{\partial}{\partial t} = \frac{W_n}{r_n}\left(\lambda \frac{\partial}{\partial \log y} - \frac{\partial}{\partial \log x}\right), \tag{22}$$

where

$$\lambda \equiv \frac{\mathrm{d}\log y}{\mathrm{d}\log \xi}, \tag{23}$$

Table 1. Dimensionless energy integral J, velocity ratios u_p/W_n, u_p/u_n, dimensionless energy constant $P/(\varrho_a c^{j+3})$ (Equation (58), (59)) and phase-plane variable Y_p for spherical flow of a dusty gas with variable energy input at the inner surface (piston) for different values of G and kp; $\gamma = 1{\cdot}4$.

β	λ	n	G	kp	J	u_p/W_n	u_p/u_n	$P/(\varrho_a c^{j+3})$	Y_p
0·5	2	−05		0	0·316610	0·846698	1·016037	73·144758	
			1	0·2	0·240652	0·809481	1·173747	69·607602	
				0·4	0·164976	0·759329	1·417415	67·704750	
			10	0·1	0·328049	0·853400	1·018200	72·857974	
				0·2	0·339297	0·860071	1·022624	72·478482	
				0·4	0·358447	0·872323	1·042135	71·341011	
			100	0·2	0·352643	0·865917	1·006974	72·820681	
				0·4	0·396779	0·888135	1·001343	72·274918	
3	0	0		0	0·248523	0·942924	1·131509	4·189805	0·222798
			1	0·2	0·183026	0·886431	1·285325	4·202392	1·192997
				0·4	0·121580	0·815541	1·522344	4·234906	4·817920
			10	0·1	0·250657	0·944533	1·126933	4·189912	0·227024
				0·2	0·251874	0·945439	1·124127	4·190103	0·240157
				0·4	0·249555	0·943654	1·127352	4·190946	0·324320
			100	0·2	0·261063	0·952270	1·107395	4·189423	0·181107
				0·4	0·274155	0·961646	1·084224	4·189186	0·144564
8	−1	1		0	0·233431	0·957175	1·148610	0·456375	
			1	0·2	0·171288	0·897124	1·300830	0·463003	
				0·4	0·113553	0·822789	1·535872	0·473017	
			10	0·1	0·234209	0·957665	1·142601	0·456726	
				0·2	0·234086	0·957382	1·138327	0·457160	
				0·4	0·229382	0·952981	1·138494	0·458414	
			100	0·2	0·242432	0·964362	1·121456	0·456574	
				0·4	0·251439	0·971283	1·095089	0·456902	

we can now write the governing equations in the following non-dimensional form:

$$\lambda y \frac{\partial h}{\partial y} + (f - x)\frac{\partial h}{\partial x} + h\left(\frac{\partial f}{\partial x} + j\frac{f}{x}\right) = 0, \tag{24}$$

$$\lambda y \frac{\partial f}{\partial y} + (f - x)\frac{\partial f}{\partial x} - \frac{\lambda}{2} f + \frac{1}{h}\frac{\partial g}{\partial x} = 0, \tag{25}$$

$$\lambda y \frac{\partial g}{\partial y} + (f - x)\frac{\partial g}{\partial x} + \frac{\Gamma g}{1 - Z_a h}\left(\frac{\partial f}{\partial x} + j\frac{f}{x}\right) - \lambda g = 0. \tag{26}$$

The decay coefficient λ is associated with the front velocity. For a similarity solution, λ must be taken constant and should be suitably connected with the energy-input parameter β, or the constant n.

According to Equation (16), a line $x = x_p$ must coincide with a particle path at the inner boundary of a blast wave, *i.e.*,

$$f(x_p) = u_p / W_n. \tag{27}$$

At the shock front, the discontinuity conditions can be written as follows:

$$h_n = \frac{1}{1 - f_n}, \tag{28}$$

$$g_n = f_n + \frac{1-Z_a}{\Gamma} y, \tag{29}$$

$$\sigma_n = \frac{{f_n}^2}{2} + \frac{(1-Z_a)}{\Gamma} y \left(f_n + \frac{1-Z_a}{\Gamma - 1} \right) \tag{30}$$

from which, by using Equations (12) and (21), we obtain conveniently

$$f_n = \frac{2(1-Z_a)}{\Gamma+1}(1-y), \tag{31}$$

$$h_n = \frac{\Gamma+1}{\Gamma - 1 + 2Z_a + 2(1-Z_a)y}, \tag{32}$$

$$g_n = \frac{2(1-Z_a)}{\Gamma+1}\left(1 - \frac{\Gamma-1}{2\Gamma} y\right). \tag{33}$$

The velocity modulus ω, which is associated more directly with the propagation velocity of the shock front, is defined as

$$\omega = \frac{\mathrm{d}\log\xi}{\mathrm{d}\log t_n} = \frac{\mathrm{d}\log r_n}{\mathrm{d}\log t_n} = \frac{W_n t_n}{r_n}. \tag{34}$$

When $\lambda \neq 0$, the front trajectory in terms of y, ξ, and $\omega \equiv t/t_0 = a_a t/R_0$, can be obtained by integrating (23) and (34) as follows:

$$\xi = \xi_0 y^{\frac{1}{\lambda}}, \quad \omega = \omega_0 \xi_0 y^{\frac{1}{(\omega_0)\lambda}}, \tag{35}$$

where ξ_0 is an integration constant. The energy integral, (19), in terms of the non-dimensional time ω and shock radius ξ, may now be put into the following form:

$$J = \frac{y(1-Z_a)}{\Gamma}\left(\frac{\omega^{\beta}}{\xi^{j+1}}\Omega + \frac{(1-Z_a)}{(j+1)(\Gamma-1)}\right), \tag{36}$$

where

$$\Omega \equiv \frac{P/n_j}{p_a {a_a}^{\beta} {R_0}^{j+1-\beta}}. \tag{37}$$

From this, by setting $\Omega = 1$, we may now define an arbitrary reference radius as follows:

$$R_0 = \left(\frac{P}{n_j p_a a_a^{\beta}}\right)^{1/(j+1-\beta)}, \quad (j+1-\beta \neq 0). \tag{38}$$

Accordingly, the non-dimensional energy integral becomes

$$J = \frac{y(1-Z_a)}{\Gamma}\left(\frac{\omega}{\xi^{j+1}} + \frac{(1-Z_a)}{(j+1)(\Gamma-1)}\right). \tag{39}$$

When $\lambda = 0$, the counter-pressure can be taken into account because the partial derivatives appearing in (24–26) vanish by multiplication with λ. As a result of a constant piston velocity, a linear law of motion is obtained in this special Case II:

$$\frac{a_a t}{R_0} = \sqrt{y}\frac{r_n}{R_0}, \tag{40}$$

where again the reference radius R_0 can be fixed arbitrarily. We may find an alternative expression of Equation (36) for Case II by using (40) instead of (35) and noting that $\beta = j+1$; hence

$$J = \frac{y(1-Z_a)}{\Gamma}\left(\frac{P y^{(j+1)/2}}{n_j p_a a_a^{j+1}} + \frac{(1-Z_a)}{(j+1)(\Gamma-1)}\right) \quad (y > 0). \tag{41}$$

3. Similarity solution

In the Cases I and III of negligible counter-pressure, *i.e.*, for $y=0$, the transformed system (24–26) including the corresponding boundary conditions permits a self-similar solution if none of the dependent variables depend on y. Accordingly, it is essential that the energy-deposition coefficient does not depend on y, except in Case II. However, for a self-similar piston problem, the piston path must be proportional to the shock path in all three cases, *i.e.*, $r_p=\alpha r_n$, so that the piston velocity is given by

$$u=u_p=\alpha W_n. \tag{42}$$

Thus, substituting Equation (35) in Equation (39) under consideration of $\omega=n+1$ as required for similarity solutions, we obtain

$$J=\lim_{y\to 0}\frac{1-Z_a}{\Gamma}(n+1)^{\beta}\xi_0^{\beta-j-1}y^{\frac{3}{2}-\frac{\beta-1}{(n+1)\lambda}-\frac{j}{\lambda}}. \tag{43}$$

Setting the exponent in Equation (43) equal to zero, we obtain to the following relations:

$$J=\frac{1-Z_a}{\Gamma}(n+1)^{\beta}\xi_0^{\beta-j-1},\quad \beta\neq j+1\qquad (n\neq 0), \tag{44}$$

$$\lambda=\frac{2(j+1-\beta)}{2+\beta}, \tag{45}$$

where $n+1=2/(\lambda+2)$, from which the exponent n is related to the energy-input parameter β through

$$n=\frac{\beta-j-1}{j+3}. \tag{46}$$

Similar expressions for a pure gas were obtained earlier by Pitkin [18]. From the above equation, we get

$$\xi_0=\left(\frac{\Gamma J}{(1-Z_a)(n+1)^{\beta}}\right)^{\frac{1}{\beta-j-1}}, \tag{47}$$

where J can then be written in terms of the dimensionless function of x as

$$J=\int_{x_p}^{1}\left(\frac{1-Z_a h}{\Gamma-1}g+h\frac{f^2}{2}\right)x^j\,\mathrm{d}x. \tag{48}$$

Thus, the trajectory of the front given by Equation (34) can now be expressed in the form

$$\frac{a_a t}{R_0}=\left(\frac{\Gamma J(n+1)^2}{1-Z_a}\right)^{\frac{1}{(n+1)(j+3)}}\left(\frac{r_n}{R_0}\right)^{\frac{1}{(n+1)}}. \tag{49}$$

From these equations, it becomes clear that $n+1$ must be greater than zero, or $n>-1$, in order to increase r_n as t increases. The expanding piston, therefore, moves in conformity with the shock front.

After setting $y=0$, the transformed equations of motion (22–24) can be written in matrix notation as

$$\mathcal{A}\frac{\mathrm{d}U}{\mathrm{d}x}=\mathcal{B}, \tag{50}$$

where $U=(f,h,g)^{\mathrm{tr}}$. The matrix $\mathcal{A}$ and the colum vector $\mathcal{B}$ can be read by inspection. The system, (50), can be solved for the derivatives $\mathrm{d}f/\mathrm{d}x$, $\mathrm{d}h/\mathrm{d}x$ and $\mathrm{d}g/\mathrm{d}x$ as follows:

$$\frac{\mathrm{d}f}{\mathrm{d}x}=\frac{\Delta_1}{\Delta}, \qquad \frac{\mathrm{d}h}{\mathrm{d}x}=\frac{\Delta_2}{\Delta}, \qquad \frac{\mathrm{d}g}{\mathrm{d}x}=\frac{\Delta_3}{\Delta}, \tag{51}$$

where Δ is the determinant of the system which is given by

$$\Delta=(f-x)\left((f-x)^2-\frac{\Gamma g}{(1-Z_a h)h}\right), \tag{52}$$

and Δ_1, Δ_2 and Δ_3 are the determinants obtained from Δ in the following form:

$$\Delta_1=(f-x)\left(\frac{\lambda}{2}f(f-x)+\left[-\lambda+\frac{j}{x}\frac{\Gamma f}{1-Z_a h}\right]\frac{g}{h}\right), \tag{53}$$

$$\Delta_2=\frac{-h}{f-x}\left(\Delta_1+\frac{j}{x}f\Delta\right), \tag{54}$$

$$\Delta_3=\frac{-g}{f-x}\left(\frac{\Gamma\Delta_1}{(1-Z_a h)}+\left[-\lambda+\frac{j}{x}\frac{\Gamma f}{(1-Z_a h)}\right]\Delta\right). \tag{55}$$

The corresponding boundary conditions in the cases $\lambda\neq 0$ in which the counter-pressure is neglected are

$$f(x_p)=\alpha, \quad f_n=g_n=\frac{2(1-Z_a)}{\Gamma+1}, \quad h_n=\frac{\Gamma+1}{\Gamma-1+2Z_a}. \tag{56}$$

As already mentioned, when $\lambda=0$, the counter-pressure p_a can also be considered so that in Case II the boundary conditions (31–33) remain valid.

From (49), (38) and (46), one obtains for the shock-front velocity

$$W_n=(n+1)\left[\frac{1}{(n+1)^2}\frac{P}{n_j\varrho_a J}\right]^{1/(j+3)}t^n. \tag{57}$$

Comparing this with $W_n=(c/\alpha)t^n$, we may express the non-dimensional energy constant $P^*=P/\varrho_a c^{j+3}$ in terms of n, α and the energy integral J as follows:

$$\frac{P}{\varrho_a c^{j+3}}=\frac{n_j}{(n+1)^{(j+1)}}\frac{J}{\alpha^{(j+3)}}. \tag{58}$$

Admittedly, this relation applies to the Cases I and III. However, one may apply Equation (58) to Case II, if y approaches zero, which corresponds to shock waves driven by a piston at zero velocity of sound (or temperature). On the other hand, the use of Equation (41) in Case II for $y>0$ leads to

$$\frac{P}{\varrho_a c^{j+3}}=\frac{n_j J}{\alpha^{(j+3)}}-\frac{n_j g_a(1-Z_a)}{(\Gamma-1)(j+1)\alpha^{j+3}} \quad (n=0). \tag{59}$$

The combination of (57), (58) and (13) with $Z=Z_a$ yields finally for the effective shock Mach number

$$\left(\frac{M_a}{M_{\mathrm{ga}}}\right)_t=\left(\frac{1-Z_a}{[(1-k_p)\Gamma/\gamma]^{1/2}}\right)\left(\frac{(1-k_p)J_0}{(1-Z_a)J}\right)^{\frac{1}{(j+3)}}=\left(\frac{1-Z_a}{[(1-k_p)\Gamma/\gamma]^{1/2}}\right)\frac{\alpha_0}{\alpha}, \tag{60}$$

where M_{ga} is the shock Mach number of the dust-free gas.

4. Results and discussion

In order to integrate the set of nonlinear ordinary differential equations (39–41), we use the Runge–Kutta fourth-order method with a variable step size. The integration has been carried out for spherical blast waves, *i.e.*, for $j=2$, starting from the shock front ($x=1$) and proceeding inwards until the piston is nearly surrounded. Furthermore, the parameters appearing in Equation (11) were assumed to apply for $\gamma=1{\cdot}4$ and $\beta_{\mathrm{sp}}=1$, respectively. The results are given for various values of the mass fraction k_p (mass concentration of the solid particles) at constant volumetric parameter G (ratio of density of the solid particles to the initial density of the gas) and vice versa.

The value of the constant λ occurring in the above equations gives rise to different cases of possible solutions, which will be discussed in the following. In addition, we also illustrated the flow behind the shock wave in the conventional phase plane by introducing the following reduced variables:

$$F=\frac{f}{x},\quad Y=\frac{\Gamma}{x^2(1-Z)}\frac{g}{h}\quad (Z\leq 1). \tag{61}$$

The physically meaningful self-similar solution extends from the shock point to the piston path without crossing a limiting characteristic (acoustic line). Thus, the range of interest in the (F,Y)-plane is

$$\frac{2(1-Z_a)}{\Gamma+1}<F<1,\quad Y>0, \tag{62}$$

in which the flow is subsonic, since

$$Y-(1-F)^2>0,\quad \text{or}\quad F\pm\sqrt{Y}>1. \tag{63}$$

From Equations (61), (28) and (29) at $x=1$, the relation for the Hugoniot curve in the phase plane is obtained for the Case II in the general form

$$Y_n=\frac{\Gamma(1-F_n)^2}{1-F_n-Z_a}\left(F_n+\frac{1-Z_a}{\Gamma}y\right), \tag{64}$$

which for the Cases I and III where $y=0$ reduces to

$$Y_n=\frac{\Gamma(1-F_n)^2F_n}{1-F_n-Z_a}. \tag{65}$$

4.1. Case I

The case of $\lambda>0$ ($n>-1$) corresponds to an expanding and decelerated piston. Since $f=f_p$, and the density approaches zero, $h=h_p=0$, for fluid particles adjacent to the piston, the singular-image points in the phase plane must be on the line $F=1$ at $Y_p=\infty$ as is obvious from Figures 1a, b, 4a, b and Table 1, where some essential flow parameters are summarized. Based on the limiting value $(\mathrm{d}f/\mathrm{d}x)_p=\lambda/\Gamma-j$ and (61), the slope of the integral curves in the phase plane on the piston is then $(\mathrm{d}Y/\mathrm{d}F)_{F=1}=+\infty$. However, because of the strong-shock assumptions, Case I may only be valid for early times when $W_n\gg a_a{}^2$.

To see the effect of the mass concentration k_p and the mass-loading G of the dust on the flow field, the radial variation of dimensionless velocity, pressure and density between shock and piston has been plotted for $k_p=0$, $k_p=0{\cdot}1$, $k_p=0{\cdot}3$, $k_p=0{\cdot}4$ and $G=1$, allowing a comparison with the dust-free case for $k_p=0$ in Figure 1a, and at $G=1$, 10, 1000 and $k_p=0{\cdot}2$ in Figure 1b. The pressure and the density increase in the radial direction while the velocity

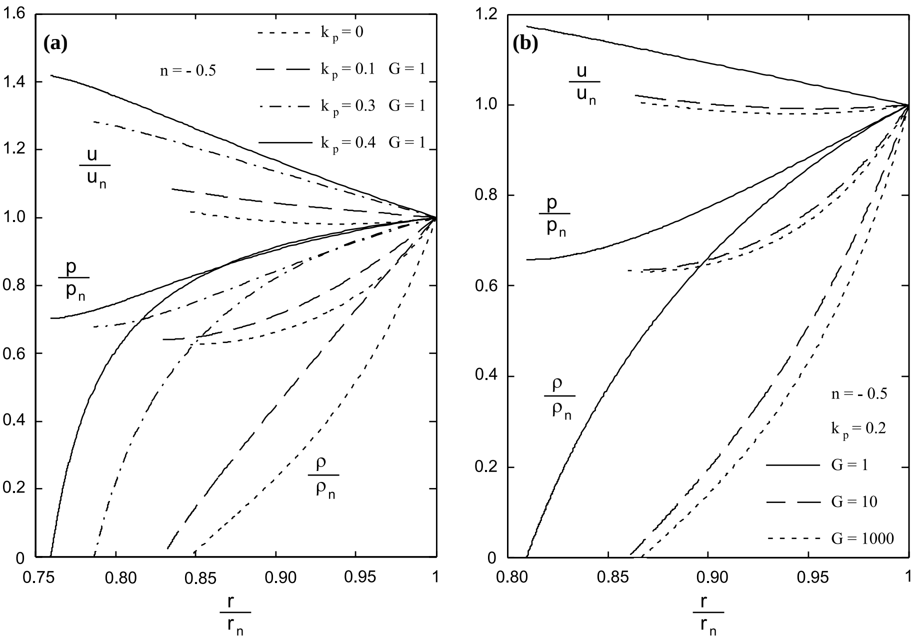

Figure 1. Non-dimensional velocity, pressure and density distribution for Case I with time exponent $n = -0{\cdot}5$: (a) for various values of k_p (mass concentration of the solid particles) and one value of G (ratio of density of the solid particles to the initial density of the gas); (b) for various values of G and one value of k_p.

decreases. This behavior, especially for the case of $k_p = 0{\cdot}4$ and $G = 1$, differs greatly from the dust-free case.

The flow field in the phase plane is shown in Figures 4a and b. The Hugoniot curve is drawn in accordance with Equation (65) as a thin line from point $F = 0$, $Y = 0$ up to the shock point F_n, Y_n which is denoted by a small circle. An interesting result is that the solution curves may reach a zero slope at the shock and later these curves show a minimum between shock front and piston face.

4.2. Case II

When $\lambda = 0$ $(n = 0)$, it follows from the similarity solution that $(\mathrm{d}f/\mathrm{d}x)_p = -j$, $(\mathrm{d}g/\mathrm{d}x)_p = (\mathrm{d}h/\mathrm{d}x)_p = 0$ and $h_p > 0$. The location of these singular points in the phase plane must be on the line $F = 1$ at $Y = Y_p$ which is not known until the problem has been solved. The slope of the integral curves in the phase plane on the piston may be evaluated through limiting processes, yielding: $(\mathrm{d}Y/\mathrm{d}F)_{F=1} = 2Y_p/(j+1)$. In this limiting case both the piston and the shock front propagate and expand with constant velocities. Thereby the piston starts its motion instantaneously from rest and the medium is adiabatically compressed in the region between these two fronts.

It should be recalled that for $\lambda = 0$, since the counter-pressure can be taken into account by Equations. (31), (32) and (33), y must not be a negligible quantity as in the Cases I and III. However, as in these cases, we attain velocity and temperature equilibrium at a short distance behind the shock front in comparison with the distance between shock and piston front, as long as we use solutions for $y \ll 1$. The corresponding plots of dimensionless velocity, pressure and density are presented in Figures 2a for $k_p = 0{\cdot}1$, $k_p = 0{\cdot}3$, $k_p = 0{\cdot}4$ and the volumetric parameter $G = 1$ at $y = 0$ and $y = 0{\cdot}01$ (thin lines), respectively, and in Figures 2b for $G = 1$, 10, 1000 and $k_p = 0{\cdot}2$ at $y = 0$ and $y = 0{\cdot}01$ (thin lines),

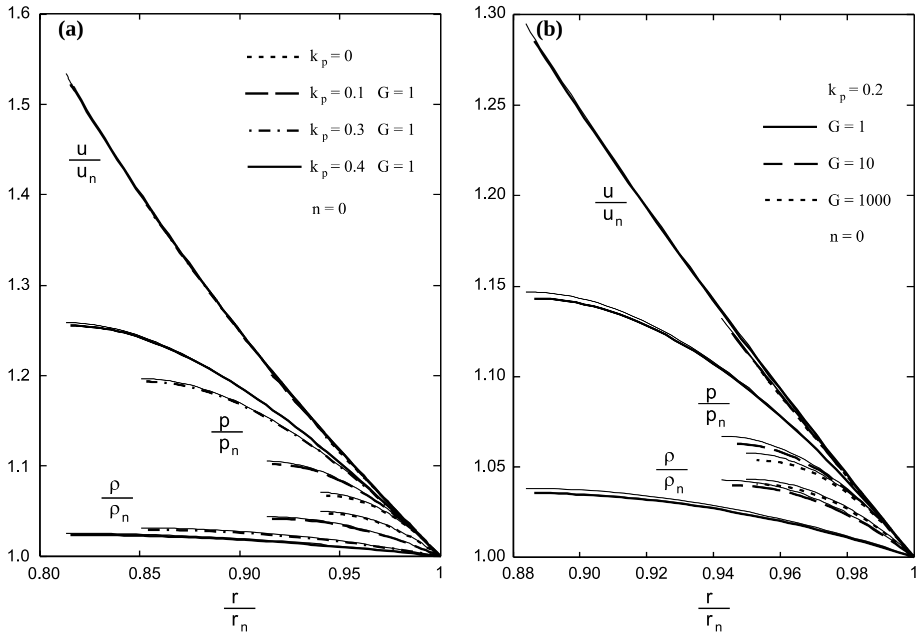

Figure 2. Non-dimensional velocity, pressure and density distribution for $n = 0$ and $1/M^2 = 0$ or $1/M^2 = 0{\cdot}01$ (thin lines): (a) for various values of k_p (mass concentration of the solid particles) and one value of G (ratio of density of the solid particles to the initial density of the gas); (b) for various values of G and one value of k_p.

respectively. In these cases pressure as well as density and velocity decrease in the radial direction. The effect of the dust-loading parameters k_p and G on the pressure and density profile is evident, except the effect on the velocity profile which can be seen from Table 1.

4.3. Case III

When $\lambda < 0$ $(n > 0)$, it follows from the similarity solution that $(\mathrm{d}h/\mathrm{d}x)_p = \infty$, and $h_p = 1/Z_a$ at the piston. The slope of the integral curves in the phase plane on the piston becomes $(\mathrm{d}Y/\mathrm{d}F)_{F=1} = +\infty$ for $k_p > 0$. In the dust-free case $h_p = \infty$ and consequently $Y_p = 0$ and $(\mathrm{d}Y/\mathrm{d}F)_{F=1} = -\infty$. This case corresponds to an expanding and continuously accelerated piston starting from rest. Both piston path and shock path converge, in the course of which the medium will be condensed, reaching a finite state $(Z = 1)$. Hence, the most significant feature of the flow field in Case III is the existence of a limiting value for the density $(h_p = 1/Z_a)$ as shown in Figure 3.

Again, the corresponding plots depicted in Figure 3a and b distinctly show the effect of the dust parameters k_p and G on the radial profiles of the velocity, pressure and density. The self-similar flow field, however, will be reached at later times when $W_n \gg {a_a}^2$.

Table 1 shows the ratios of the piston velocity u_p to the propagation velocity of the shock W_n, on the one hand, and to the particle velocity of the mixture immediately behind the shock u_n, on the other, in all three cases. In all these cases the dimensionless energy integral J and the velocity ratio u_p/W_n decrease as the dust-mass fraction k_p for $G = 1$ increases, while they slightly increase for values of $G \geq 100$. The velocity ratio of u_p/u_n acts just the opposite way; it increases with increasing k_p for $G = 1$, while it decreases slightly for values of $G \geq 100$ (Figures 4–6).

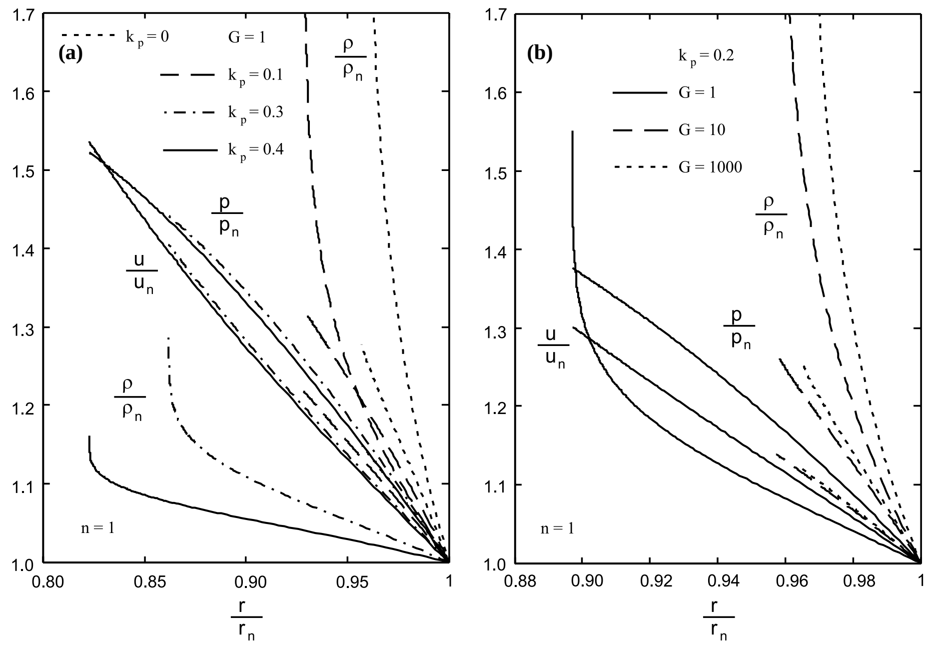

Figure 3. Non-dimensional velocity, pressure and density distribution for Case III with time exponent $n = 1$: (a) for various values of k_p (mass concentration of the solid particles) and one value of G (ratio of density of the solid particles to the initial density of the gas); (b) for various values of G and one value of k_p.

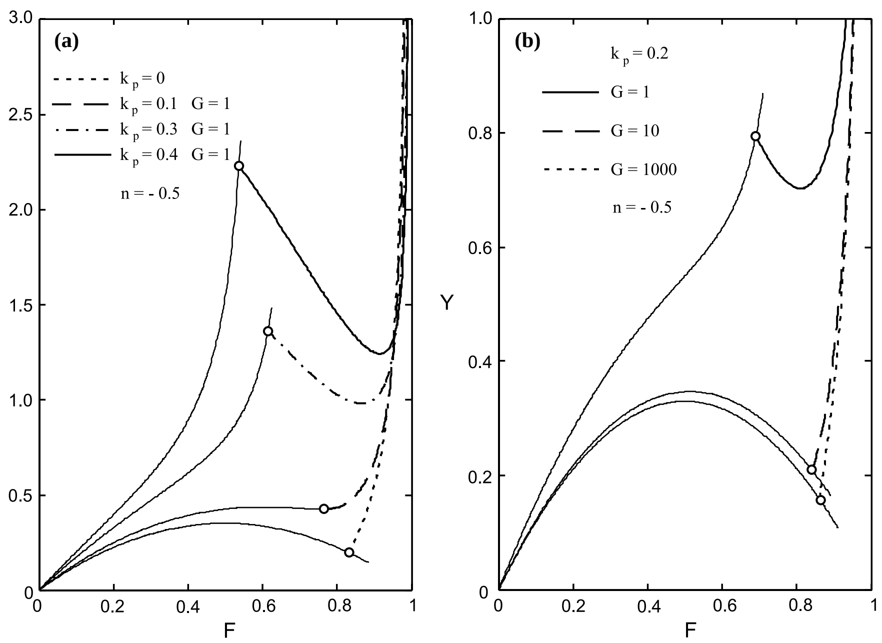

Figure 4. Solutions in the phase plane for Case I with time exponent $n = -0{\cdot}5$: (a) for various values of k_p (mass concentration of the solid particles in the mixture) and constant values of G (ratio of density of the solid particles to the initial density of the gas); (b) for various values of G and one value of k_p.

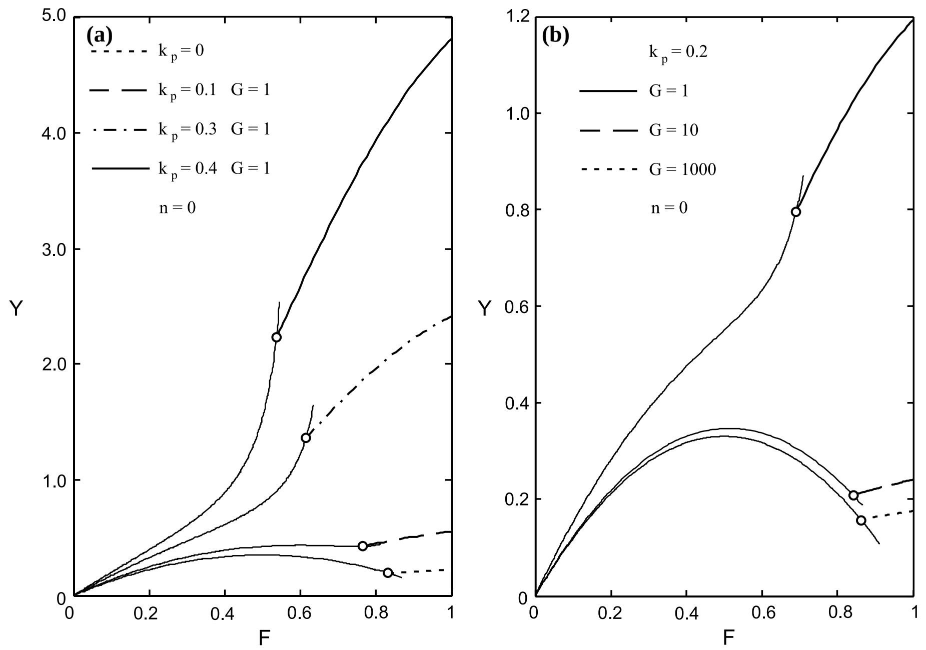

Figure 5. Solutions in the phase plane for Case II with time exponent $n = 0$: (a) for various values of k_p (mass concentration of the solid particles in the mixture) and constant values of G (ratio of density of the solid particles to the initial density of the gas); (b) for various values of G and one value of k_p.

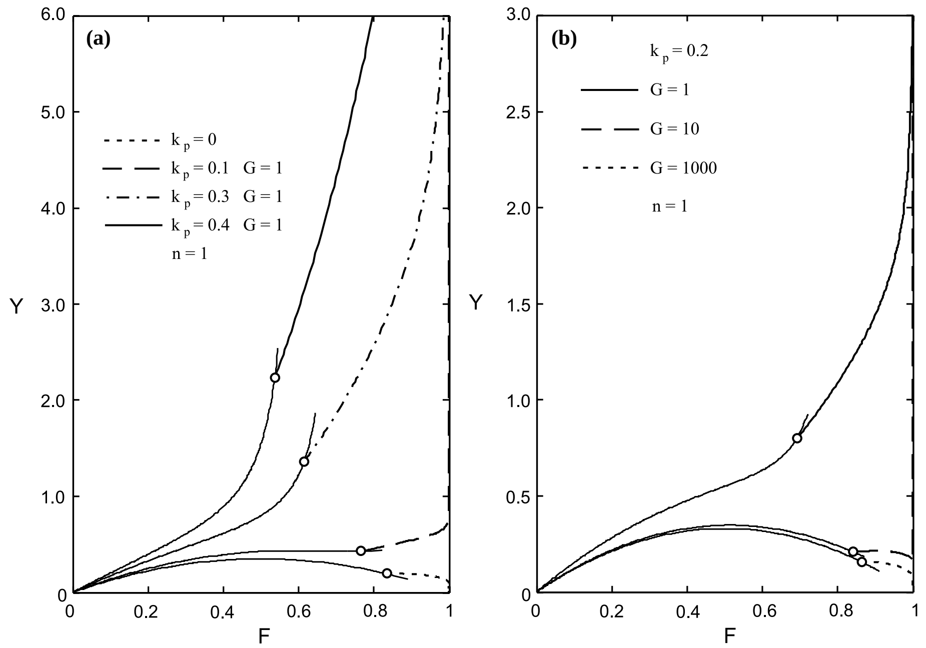

Figure 6. Solutions in the phase plane for Case III with time exponent $n = 1$: (a) for various values of k_p (mass concentration of the solid particles in the mixture) and constant values of G (ratio of density of the solid particles to the initial density of the gas); (b) for various values of G and one value of k_p (ratio of density of the solid particles to the initial density of the gas).

Note that the initial sound speed a_a of the mixture, defined by (13) where $Z = Z_a$, behaves also inversely, it increases with increasing k_p for $G = 1$, while it decreases approximately linearly for values of $G \geq 100$.

When the energy-input parameter β approaches zero, or when $n = -(j+1)/(j+3)$, the system of equations (39–41) leads to the limiting case for instantaneous energy input in a dusty gas.

The ratio of the effective shock Mach number M_a/M_{ga} for a dusty gas to that for dust-free gas is depicted in Figures 7. A comparison of the shock Mach numbers W_n/a_a at the same time, Equation (60), reveals that W_n/a_a decreases with increasing k_p for lower values of G (*e.g.*, $G = 1$) and increases for higher values of G (*e.g.*, $G \geq 10$). In other words, the shock becomes weaker with increasing k_p for lower values of G and stronger for higher values of G. A plausible explanation is given by the decrease of the energy integral with increasing k_p for $G = 1$ and by its increase with increasing G. Another simple explanation for this behavior is given by the fact that an increase of shock velocity is accompanied by an increase of the sound velocity for $G = 1$ and, oppositely, a decrease of the shock velocity for $G \geq 10$ is more than balanced by a decrease of the sound velocity, respectively. It should also be remembered in this context what was said in the previous discussion about the deviation of the dusty gas from the dust-free gas (on the end of Section 2.1) in which compressibility plays an overriding role towards a physical interpretation. The sound speed is related to the compressibility of a gas. The presence of solid particles in the mixture decreases the compressibility and thus, on the one hand, explains why the speed increases. But, on the other hand, the dust loading may increase the inertia and thus decrease the speed of sound.

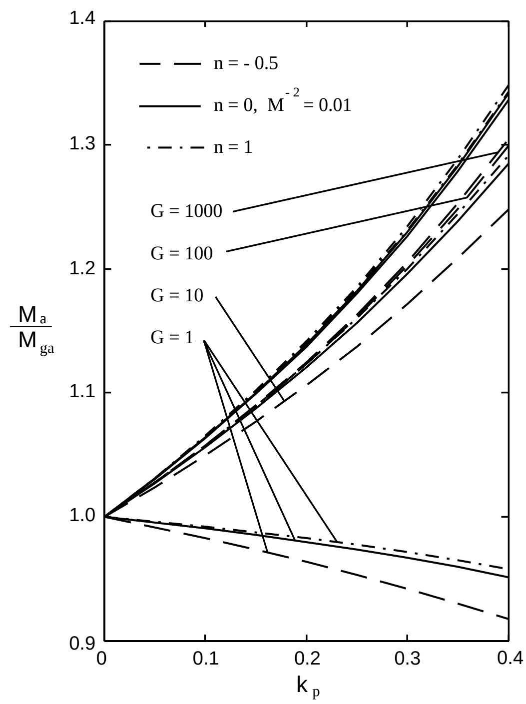

Figure 7. Variation of the effective shock Mach number M_a with mass concentration of the solid particles in the mixture k_p for various values of G. M_{ga} is the shock-Mach number of the dust-free (perfect) gas.

5. Concluding remarks

A self-similar solution for blast waves of variable energy propagating into a dusty gas at rest has been given here under the condition that the total energy of the flow between the front and an inner expanding surface or piston is increasing with time according to a power law. Three different cases were covered with respect to parameters describing the increase of energy or the piston velocity: the first corresponds to a decelerated piston, the second to constant piston velocity and the third to a continuously accelerated piston starting from rest. Necessary conditions for the existence of similarity solutions for strong shock waves, as well as for those of arbitrary strength, have been obtained. The results were compared in all three cases with those of a dust-free gas. It was found that the dusty gas can have significant effects on the variation of sound speed, shock velocity, shock Mach number (shock strength), density and pressure as well as on variation of the paths of shock and piston in the time-space domain. The correspondence between the piston problem and the self-similar case of variable energy deposition in the flow field could be expressed on the one hand by a non-dimensional energy constant P^*, and on the other through a relation between n and the energy-input parameter β.

References

1. G.I. Taylor, The air wave surrounding an expanding sphere. *Proc. R. Soc. London* A 186 (1946) 273.
2. L.I. Sedov, *Similarity and Dimensional Methods in Mechanics*. New York: Academic Press (1959) 363pp.
3. R.A. Freeman, Variable energy blast wave. *J. Phys. D, App. Phys.* (1968) 1697–1710.
4. M.N. Director and E.K. Dabora, Predictions of variable-energy blast waves, *AIAA J.* 15 (1977) 1315–1321.
5. E.K. Dabora, Variable energy blast waves. *AIAA J.* 10 (1972) 1384–1386.
6. R.H. Guirgius, A.K. Oppenheim and M.M. Kamel, Self-similar blast waves supported by variable energy deposition in the flow field. *Progr. Astron. Aeron.* 75 (1981) 178–192.
7. J.P. Vishwakarma, Propagation of shock waves in a dusty gas with exponential varying density. *Eur. Phys. J. B* 16 (2000) 369–372.
8. R. Miura and I.I. Glass, Development of the flow induced by a piston moving impulsively in a dusty gas. *Proc. R. Soc. London* A 3 (1985) 295–309.
9. T. Saito, M. Marumoto and K. Takayama, Numerical investigations of shock waves in gas-particle mixtures. *Shock Waves* 13 (2003) 299–322.
10. S. I. Pai, S. Menon and Z.Q. Fan, Similarity solution of a strong-shock wave propagation in a mixture of gas and dusty particles. *Int. J. Engng. Sci.* 18 (1980) 1365–1373.
11. S. I. Pai and S. Luo, *Theoretical and Computational Dynamics of a Compressible Flow*. New York: Van Nostrand Reinhold and Science Press (1991) 699 pp.
12. F. Higashino and T. Suzuki, The effect of particles on blast waves in a dusty gas. *Z. Naturforsch.* 35a (1980) 1330–1336.
13. G. Rudinger and A. Chang, Analysis of nonsteady two-phase flow. *Phys. Fluids* 7 (1964) 1747–1754.
14. F.E. Marble, Dynamics of dusty gases. *A Rev. Fluid Mech.* 2 (1970) 397–446.
15. F. Higashino, Characteristic method applied to blast waves in a dusty gas. *Z. Naturforsch.* 38a (1983) 399–406.
16. J.H. Geng and H. Grönig, Dust suspensions accelerated by shock waves. *Exp. Fluids* 28 (2000) 360–367.
17. A.K. Oppenheim, A.L. Kuhl, E.A. Lundstrom and M.M. Kamel, A parametric study of self-similar blast waves. *J. Fluid Mech.* 52 (1972) 657–682.
18. E.T. Pitkin, Perturbation solutions for variable energy blast waves. *Acta Astronaut.* 4 (1977) 1137–1158.